Check for updates

Suicidal Phenotype of Proofreading-Deficient Herpes Simplex Virus 1 Polymerase Mutants

Marika Brunialti,[a] Thomas Höfler,[a] Mariana Nascimento,[a] Jakob Trimpert[a]

[a]Institut für Virologie, Freie Universität Berlin, Berlin, Germany

Marika Brunialti and Thomas Höfler contributed equally to this article. Author order was determined alphabetically.

ABSTRACT Herpes simplex virus 1 (HSV-1) encodes a family B DNA polymerase (Pol) capable of exonucleolytic proofreading whose functions have been extensively studied in the past. Early studies on the *in vitro* activity of purified Pol protein found that the enzymatic functions of the holoenzyme are largely separate. Consequently, exonuclease activity can be reduced or abolished by certain point mutations within catalytically important regions, with no or only minor effects on polymerase activity. Despite unimpaired polymerase activity, the recovery of HSV-1 mutants with a catalytically inactive exonuclease has been so far unsuccessful. Hence, mutations such as D368A, which abolish exonuclease activity, are believed to be lethal. Here, we show that HSV-1 can be recovered in the absence of Pol intrinsic exonuclease activity and demonstrate that a lack of proofreading causes the rapid accumulation of likely detrimental mutations. Although mutations that abolish exonuclease activity do not appear to be lethal, the lack of proofreading yields viruses with a suicidal phenotype that cease to replicate within few passages following reconstitution. Hence, we conclude that high replication fidelity conferred by proofreading is essential to maintain HSV-1 genome integrity and that a lack of exonuclease activity produces an initially viable but rapidly suicidal phenotype. However, stably replicating viruses with reduced exonuclease activity and therefore elevated mutation rates can be generated by mutating a catalytically less important site located within a conserved exonuclease domain.

IMPORTANCE Recovery of fully exonuclease-deficient herpes simplex virus 1 (HSV-1) DNA polymerase mutants has been so far unsuccessful. However, exonuclease activity is not known to be directly essential for virus replication, and the lethal phenotype of certain HSV-1 polymerase mutants is thus attributed to factors other than exonuclease activity. Here, we showed that the recovery of a variety of exonuclease-deficient HSV-1 polymerase mutants is possible and that these mutants are initially replication competent. We, however, observed a progressive loss of mutant viability upon cell culture passaging, which coincided with the rapid accumulation of mutations in exonuclease-deficient viruses. We thus concluded that a lack of DNA proofreading in exonuclease-deficient viruses causes an initially viable but rapidly suicidal hypermutator phenotype and, consequently, the extinction of mutant viruses within few generations following recovery. This would make the absence of exonuclease activity the primary reason for the long-reported difficulties in culturing exonuclease-deficient HSV-1 mutants.

KEYWORDS DNA polymerase, DNA replication, error prone, error threshold, exonuclease, herpes simplex virus, hypermutation, lethal mutagenesis, mutation, proofreading

Herpes simplex virus 1 (HSV-1) is a human alphaherpesvirus and member of the large *Herpesviridae* family (1). To achieve high replication fidelity, all members of the order *Herpesvirales* encode a viral replication machinery, including a family B DNA polymerase (Pol). In HSV-1, this enzyme is encoded by the open reading frame (ORF) unique long 30
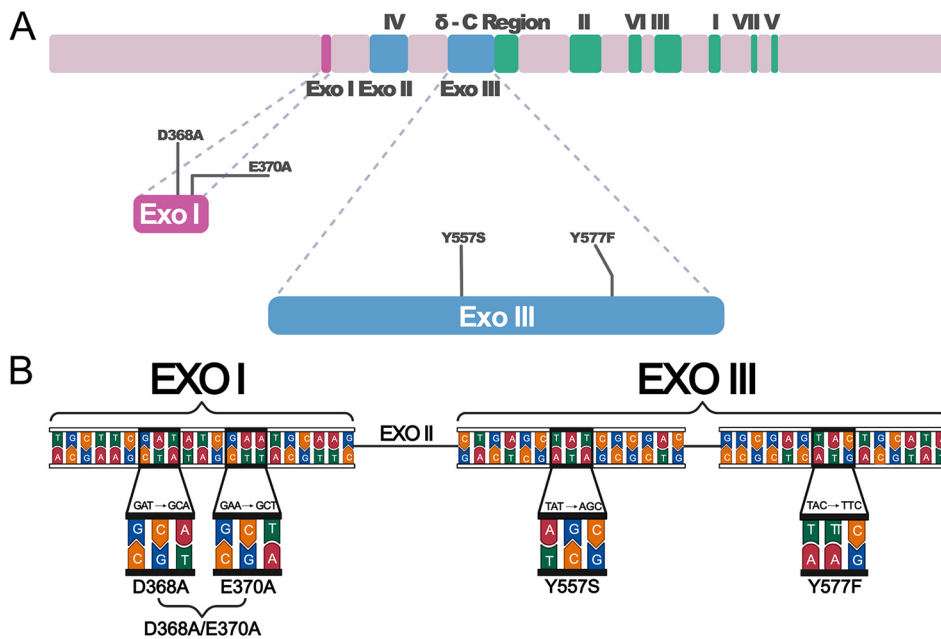
FIG 1 Mutations introduced into the HSV-1 DNA polymerase gene. (A) Schematic representation of HSV-1 UL30, the polymerase gene with highlighted functional domains. (B) To generate Exo-deficient Pol mutants used in this study, catalytically important residues within conserved Exo domains I and III were mutated based on a previously published mutational analysis of HSV-1 Pol (9).

(UL30). Family B polymerases coordinate two opposite enzymatic functions in one holo-enzyme and carry a 5′–3′ polymerase domain for DNA replication activity and a 3′–5′ exo-nuclease (Exo) domain capable of exonucleolytic proofreading (2). Structurally, herpes-virus family B polymerases share seven conserved polymerase domains, named I to VII (according to the degree of conservation), the δ-C region, and three exonuclease domains, named Exo I to Exo III (3, 4). The first conserved exonuclease domain (Exo I) does not overlap any other part of the enzyme with known catalytic function, while Exo II and Exo III overlap the conserved Pol domain IV and the δ-C region, respectively (Fig. 1A). Several studies inves-tigating the role of Exo in HSV-1 Pol have been carried out in the past (5–10). A hallmark study on the *in vitro* activity of HSV-1 Pol identified regions in the Pol gene where Exo activ-ity can be manipulated with no or only minor effect on Pol activity. However, a strong inter-dependence of both functions is apparent in other regions of the enzyme. Specifically, mutations within Exo II and Exo III domains typically affect both enzymatic functions simulta-neously (9). Mutants that show strong reduction of polymerase activity are not able to repli-cate DNA efficiently and thus yield nonviable viruses (5). On the other hand, specific muta-tions targeting the exonuclease catalytic core within Exo I abrogate Exo activity entirely by preventing the coordination of the Mg^{2+} required for catalytic activity (9, 11) but without compromising the efficiency of DNA replication. Previously, several studies on the HSV-1 Pol D368A mutant, an Exo I mutant in which exonuclease activity is eliminated without any neg-ative effect on DNA synthesis, found the substition to be lethal, as reconstitution of mutant viruses in noncomplementing cell lines failed (9, 10, 12, 13). It has been proposed that the reason for the observed lethal phenotype is not the lack of Exo activity but rather a not yet fully characterized effect of the mutation on expression of the holoenzyme (13). Recently, we have constructed a series of Exo-deficient Pol mutants in Marek's disease virus (MDV), an oncogenic alphaherpesvirus of chicken classified as gallid alphaherpesvirus 2 (GaAHV-2) (14). We found catalytically important residues to be highly conserved between MDV and HSV-1 (15). Moreover, we determined that the *in vitro* enzymatic activity of purified MDV Exo I or Exo III mutant Pol is in good agreement with published reports "on homologous HSV-1 Pol mutations." However, in contrast to literature published on HSV-1 Pol mutants, we found both MDV Exo I and Exo III Pol mutants to be viable upon reconstitution in

noncomplementing cells. Importantly, this does include D358A, the D368A homologue, which could not be reconstituted in the case of HSV-1. However, we found that Exo-deficient mutants such as D358A displayed a suicidal phenotype and typically ceased forming viable virus progeny within few passages following reconstitution. This suicidal phenotype could be linked to the rapid accumulation of mutations in viral genomes; we thus surmise that the observed aggregation of mutations, facilitated by a lack of exonucleolytic proofreading in Exo-deficient mutants, is causal for the observed loss of replication capacity. In this case, the excessively error-prone genome replication would cause viral genomes to accumulate deleterious mutations faster than they can be cleared, resulting in steep declines in replicative fitness, thus presenting the primary reason for the successive loss of viral viability observed by us. A situation in which a viral population continues to hypermutate to a degree which renders the vast majority of its progeny unfit is described as lethal mutagenesis. Lethal mutagenesis requires that, by means of deleterious mutation, an infectious virus particle creates on average fewer than one infectious offspring (16). This scenario is well described for RNA viruses and has been exploited as an antiviral therapy concept (17, 18). Based on our previous findings for MDV and accounting for the highly conserved nature of alphaherpesvirus replicative DNA polymerases, we hypothesized a lethal mutagenesis-like scenario for proofreading-deficient HSV-1 Exo mutants. To elucidate the phenotype of Exo-deficient HSV-1 Pol mutants, we constructed three Exo I mutants, D368A, E370A, and D368A/E370A, which are expected to abolish exonuclease activity, and two Exo III mutants, Y557S and Y577F, which are expected to retain some amount of residual exonuclease activity (9). In this study, we investigate the phenotype of these mutants; our results suggest that all Exo mutants presented here can be reconstituted in noncomplementing cells while most of them exhibit a suicidal phenotype similar to what we observed for MDV mutant homologues.

RESULTS

Exonuclease-deficient HSV-1 Pol mutants are initially viable in cell culture. Based on previous results obtained for MDV (GaAHV-2) polymerase mutants (14), we hypothesized that point mutations within the 3′–5′ exonuclease domain of the viral DNA polymerase are not lethal but increase mutation rates, in some cases to an extent that yields viruses with suicidal phenotypes. These phenotypes would be caused by lethal mutagenesis due to the accumulation of deleterious mutations and increased genetic load. To test this hypothesis for HSV-1, we generated mutants harboring mutations in Exo I and Exo III (Fig. 1B) using a reverse genetics system (19). Exo I mutants D368A (GAT→GCA), E370A (GAA→GCT), and D368A/E370A (GAT→GCA/GAA→GCT) have been described as catalytically inactive (9) due to their inability to coordinate the catalytically required Mg^{2+} ion. On the other hand, Exo III mutants Y557S (TAT→AGC) and Y577F (TAC→TTC) are expected to retain a certain amount of exonuclease activity (9). We were able to reconstitute all HSV-1 Pol mutants that were subjects of this study by transfecting Vero cells with the respective virus DNA. In all cases, a visible cytopathic effect (CPE) became apparent within 48 h posttransfection, but the focus sizes differed considerably between mutants (Fig. 2A). Upon serial passage, differences between mutants became even more obvious, with only Y557S retaining a typical HSV-1 plaque phenotype, while for all other mutants, infection foci did not extend to more than a few cells by passage II (pII; see "Infection of cells and propagation of virus" for an explanation of the passage numbers) (Fig. 2B; see Fig. S1 in the supplemental material).

Viral reproduction is greatly impaired in most Pol mutants. In our attempts to characterize the phenotype of Pol mutant viruses, we also observed a decrease in the number of infection foci for all mutants except Y557S over passages. To investigate if the reduction in focus size as well as the decrease in focus numbers is due to a global decrease in viral reproduction, we quantified viral genome copies in supernatants collected from infected cell monolayers at p0 to pV via quantitative PCR (qPCR) (Fig. 2B). Viral genome copy numbers of all mutants except Y557S were several orders of magnitude lower than that of the parental wild type (WT) in all passages following reconstitution, with a steep decrease for most mutants from pI to pII. Of note, all Exo I mutants and the Exo III Y577F mutant behaved similarly, while the Y557S mutant was indistinguishable from the WT.
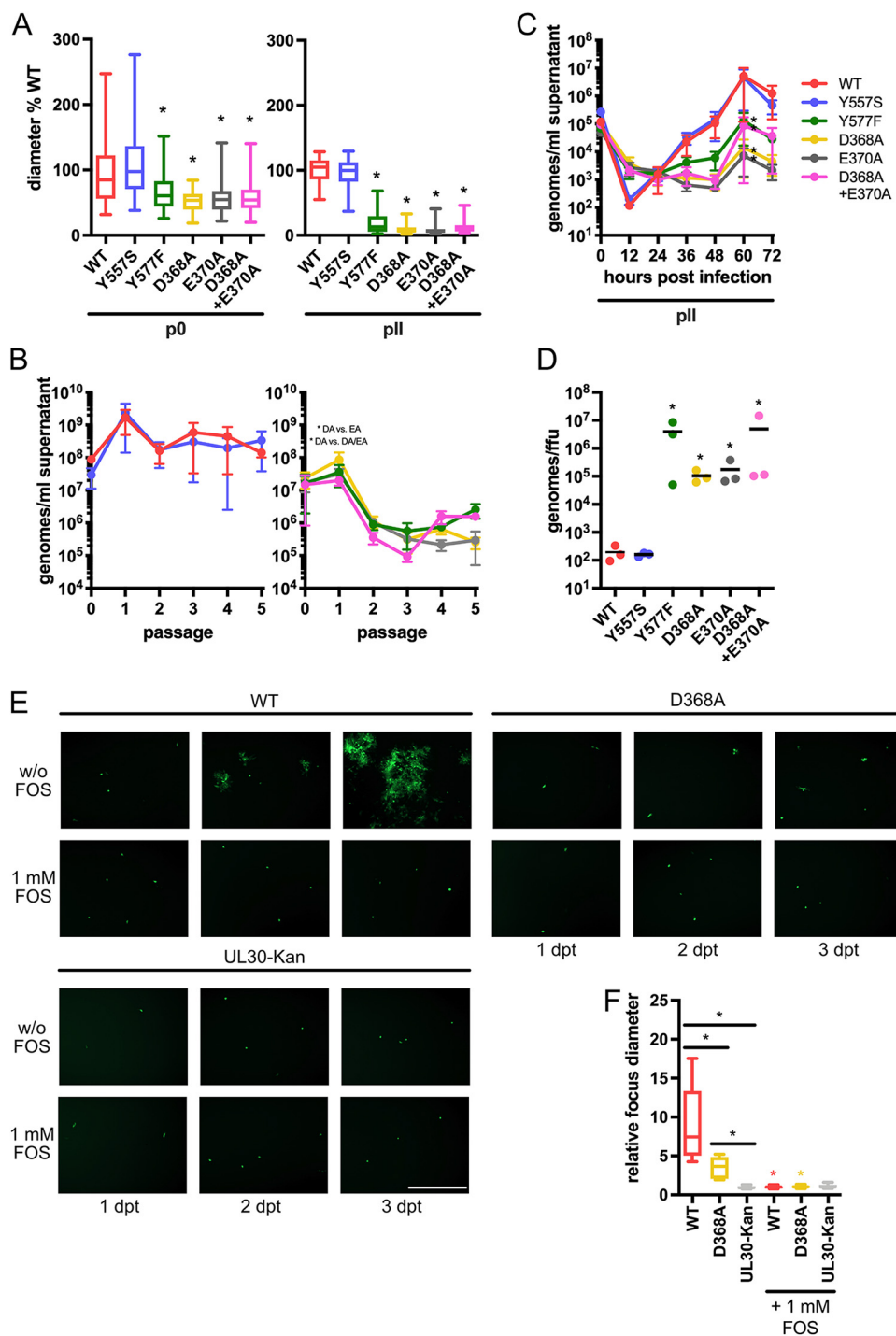
FIG 2 Exo I and Exo III Y577F mutants display severe growth deficits. (A) Focus sizes in relation to the respective WT control are shown for p0 (left) and pII (right). (B) Endpoint titers for DNA copy numbers of passaged viruses measured by qPCR. WT and Y557S (left) were, from pI onwards, passaged by infection of fresh cells with 25 μL of supernatant, whereas all other viruses (right) were passaged by splitting infected cells 1:3 for all passages. (C) Multistep growth kinetics of viruses measured at the indicated time points via qPCR. (D) Genome/FFU ratios for p0 stocks measured by qPCR and focus assay. (E) Images of growing foci taken with a Zeiss Axio Vert.A1 inverted fluorescence microscope 1, 2, and 3 days posttransfection. Scale bar, 500 μm. (F) Relative focus diameters 3 days posttransfection with or without foscarnet (FOS; 1 mM) treatment. Focus areas were measured using ImageJ and transformed into diameters. Diameters were normalized to those of WT foci treated with FOS. Analysis of variance (ANOVA) was performed for all data sets. Focus size assays and genome/FFU measurements were analyzed by one-way ANOVA followed by Dunnett's multiple-comparison test; endpoint titer and multistep growth curves were analyzed by two-way ANOVA followed by Tukey's multiple-comparison test. An asterisk indicates significant ($P < 0.05$) differences as indicated or in comparison to the WT if not further specified. Colored asterisks in panel F indicate significant ($P < 0.05$) differences in results in comparison to those of the respective untreated viruses.
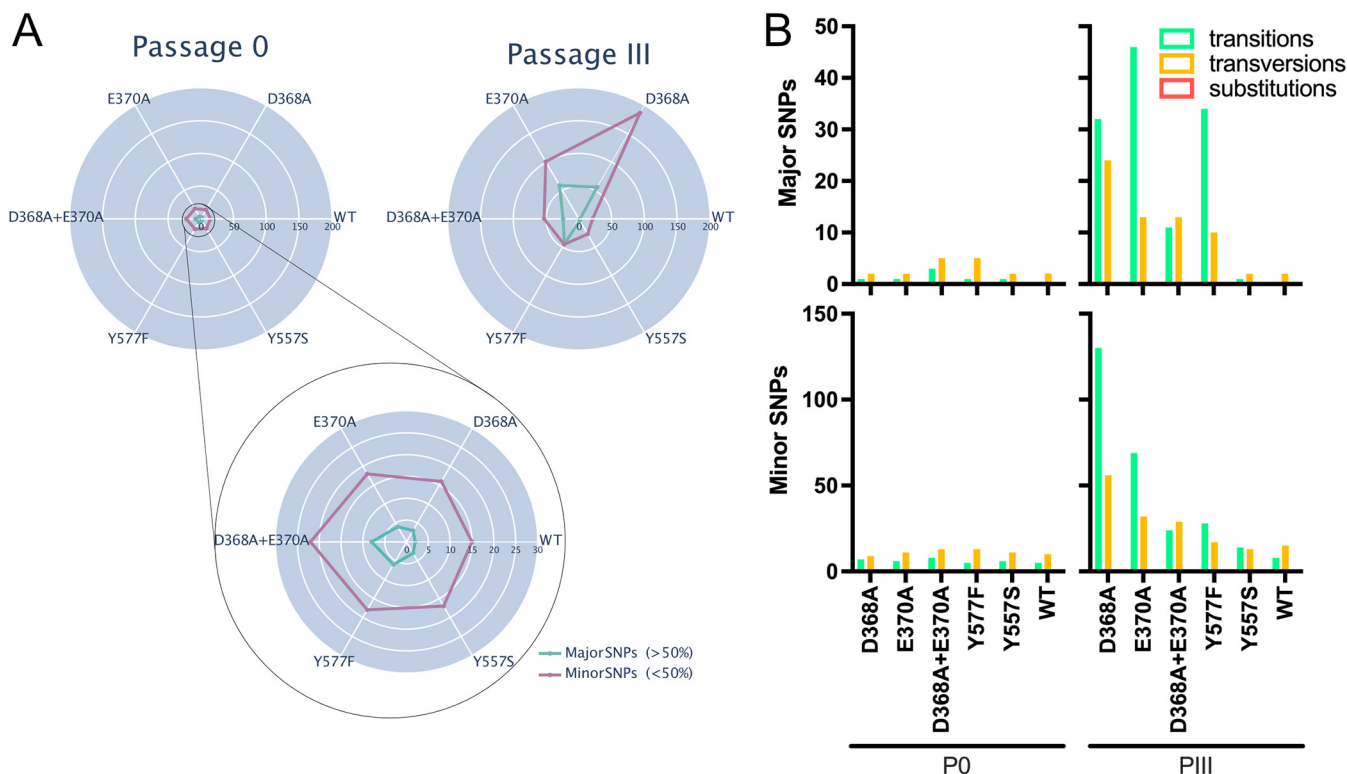
FIG 3 Exo I and Exo III Y577F mutants drastically increase mutation frequencies. (A) SNP counts broken down to major (allele frequencies above 50%) and minor (allele frequencies below 50%) for all viruses at p0 and pIII. SNPs were included if the allele frequency was greater than 5%. (B) Major and minor SNPs of p0 and pIII viruses displayed according to the type of nucleotide exchange.

Accounting for the weak growth of all Pol mutants except Y557S, we were unable to passage these mutants using an inoculum similar to that for the WT and the Y557S mutant. We thus aimed to provide a more standardized assessment of virus growth using multistep growth kinetics of viruses at pII, in which we measured viral genome copies in the supernatant resulting from infection with a standardized inoculum of 200 focus-forming units (FFU) per virus (Fig. 2C). Results confirmed decreased viral reproduction in Exo I and Y577F mutants compared to that of the WT and Y557S, which again showed very similar growth. Additionally, Exo I and Y577F hypermutators drastically increased the genome-to-FFU ratios compared to those of the WT and Y557S, indicating that genomes are less likely to be associated with infectious virions (Fig. 2D). The horizontal spread of infection foci is highly dependent on Pol activity, as treatment with foscarnet (FOS; herpesvirus polymerase inhibitor) abolishes plaque formation similar to the disruption of UL30 itself (Fig. 2E and F). Overall, our results reflected the notion that the Y557S mutant replicates similarly to parental WT virus while all other Pol mutants are significantly impaired in growth.

Mutational load is drastically increased in most Pol mutants. Along with progressive growth deficits, we observed massively increased mutation frequencies in Exo mutants in comparison to those of the WT (Fig. 3A; Table S2). At p0, the overall numbers of mutations in all tested viruses were similar, although major genetic variants (single nucleotide polymorphisms [SNPs] with allele frequencies over 50%) were slightly less abundant in the WT and Y557S. After three passages, this difference became distinct when most Exo mutants accumulated double the number of minor genetic variants (SNPs with allele frequencies below 50%) in comparison to that of the WT and Y557S. Importantly, major variants again diverged more drastically, with the WT and Y557S displaying 10 times fewer SNPs than the most conservative hypermutator (D368A/E370A).

Next, we investigated whether the lack of exonucleolytic proofreading influences the type of mutations observed by us. Generally, nucleotide changes can be of two types: transitions if pyrimidine or purine bases are replaced by other pyrimidine or purine bases, respectively, and

transversions if pyrimidine changes to purine or vice versa (20). All tested viruses show a higher level of transversions at p0 in minor and major variants alike (Fig. 3B). Upon passaging, the spectrum of mutations observed in most hypermutators shifted toward a higher level of transitions. The WT and Y557S display the same distribution of mutations at both passages, with higher levels of transversions and overall higher genetic stability compared to all other Pol mutants.

Since HSV-1 features a large yet densely packed genome with about 80 to 200 ORFs (21), many of the mutations observed by us were located within coding regions. To test if the rapid accumulation of mutations in most Exo mutants could be responsible for the progressive growth deficit observed by us, we examined changes in protein coding genes more closely. At p0, silent and nonsilent mutations were fairly balanced in the minor variants, whereas all mutations in major variants were silent (Fig. 4A). In contrast, results from pIII again clearly set our strong hypermutators apart from the WT and Y557S. Not only were mutations in coding regions in Exo I and Y577F mutants more abundant, they were also enriched for amino acid changes in minor and major variants alike, as similar levels of silent and nonsilent mutations could be detected. On the other hand, not only did the WT and Y557S show fewer mutations in coding regions in general, but minor and major variants also featured lower nonsilent-to-silent mutation ratios. Of note, no amino acid-changing mutation became dominant by pIII in WT and Y557S viruses. Further analysis of amino acid-changing mutations by SIFT prediction (22) suggests that many of them have deleterious consequences, especially in major variants (Fig. 4B).

Deleterious mutations in Exo I and Y577F mutant pIII populations occurred in different proteins that are important for viral replication (Fig. 4C). These include proteins involved in DNA metabolism (DNA polymerase UL30/42, 5′–3′ exonuclease UL12, and single-strand binding protein UL29, etc.) (23, 24), structural proteins (glycoproteins UL10/27/US8 and capsid proteins UL18/19/26/26.5) (25, 26), and others. Only two deleterious mutations occurred in Y557S minor variants by pIII, which very distinctly affect tegument proteins (UL/36/47) (27). No deleterious mutations could be detected for WT or Y557S major variants.

In line with our hypothesis that random hypermutation caused by a lack of HSV-1 Pol proofreading causes the elevated mutation frequencies observed for the mutants described here, we found no apparent mutational hot spots in genomes analyzed up to pIII.

Exo III Y557S mutant maintains stable growth at elevated mutation frequencies. Although we tried to maintain virus replication by passaging large amounts of infected cells and supernatants, Y577F and all Exo I mutants ceased to cause visible CPE beyond pIII in three replicate trials. On the other hand, Y557S showed stable growth but accumulated only slightly more mutations than the WT. We thus decided to further passage those two viable viruses to determine whether Y557S would accumulate a higher mutational load while still maintaining WT-like growth (Fig. 5A). Indeed, Y557S grew just like the WT at passage X (pX), as determined by multistep growth kinetics (Fig. 5B). On the other hand, plaques measured for pX at 2 days postinfection (dpi) showed significantly larger diameters produced by Y557S replicate 3 than by WT replicate 1, although all viruses produced increased plaque sizes over passaging time (Fig. 5C). Apart from plaque sizes, plaque phenotypes also changed predominantly to syncytia in the Y557S mutant and partially in WT replicate 2 (Fig. 5D).

Overall, Y557S accumulated slightly more mutations than the WT (Fig. 6A). Nucleotide change type distributions in the WT and the Y557S mutant were similar at pX, with transversions dominating over transitions in minor variants and transitions dominating over transversions in major variants (Fig. 6B). The WT and Y557S featured more mutations in protein coding regions at pX than at pIII, with elevated nonsilent-to-silent mutation ratios in major variants and more silent changes in minor variants (Fig. 6C). Most of those mutations were neutral (Fig. 6D). Deleterious mutations observed at pX affected again very distinct groups of proteins like tegument (UL36/46/48), structural proteins (UL27/53 and US6/7/8), and proteins involved in DNA metabolism (UL12/23/30) (Fig. 6E).

DISCUSSION

Mutation rates are delicate to balance: while mutations are required for adaptation and prerequisite to evolution, they can interfere with molecular functionality and may
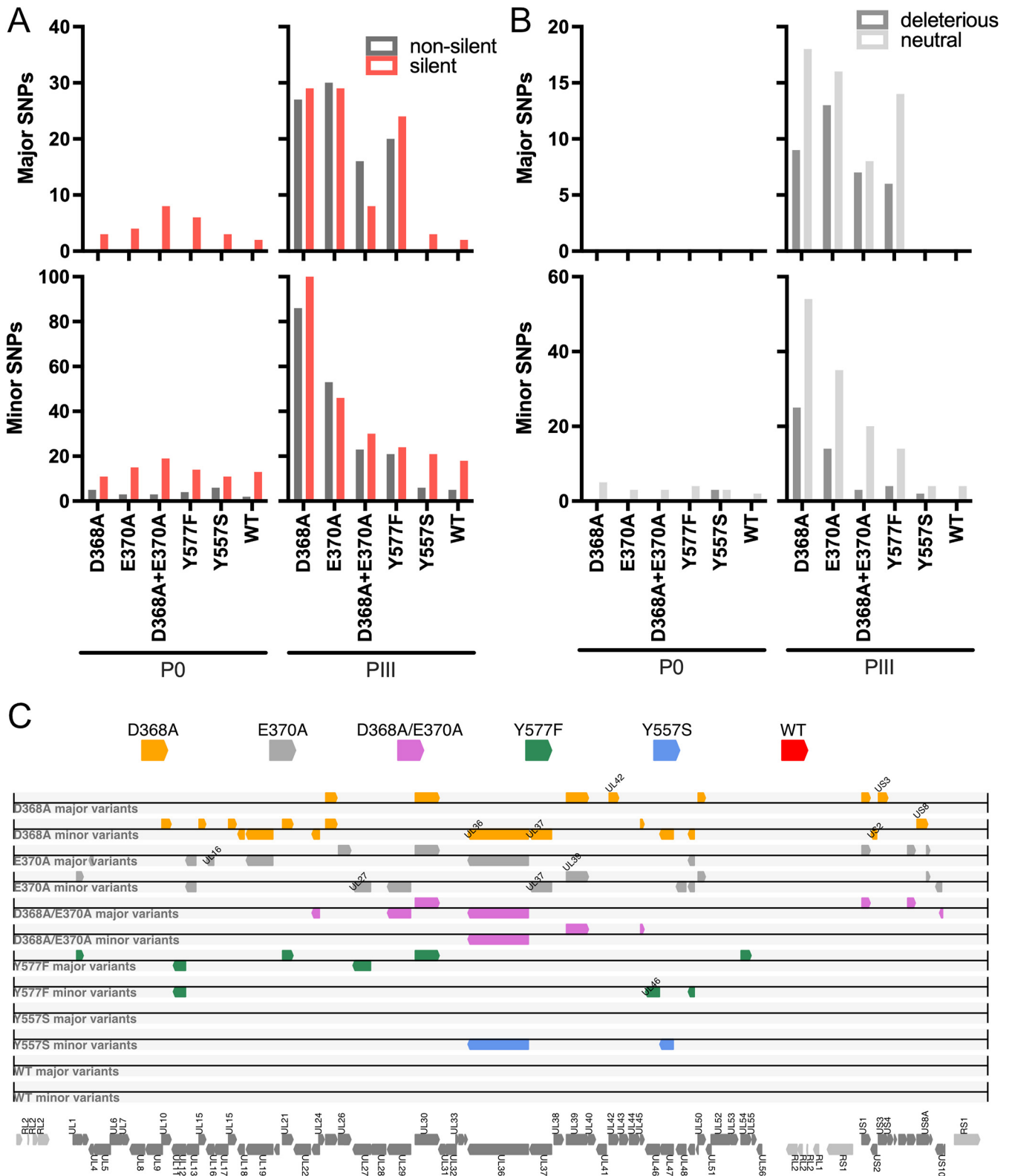
FIG 4 Hypermutators accumulate nonsilent, deleterious mutations in essential gene sets. (A) Major and minor SNPs in protein coding regions of p0 and pIII viruses grouped as silent or nonsilent according to their effects on an amino acid level. (B) Nonsilent mutations from panel A into deleterious and neutral mutations according to SIFT predictions. (C) Genes affected by deleterious major or minor mutations at pIII, respectively, are depicted. Genes labeled with their respective names feature more than one deleterious mutation.
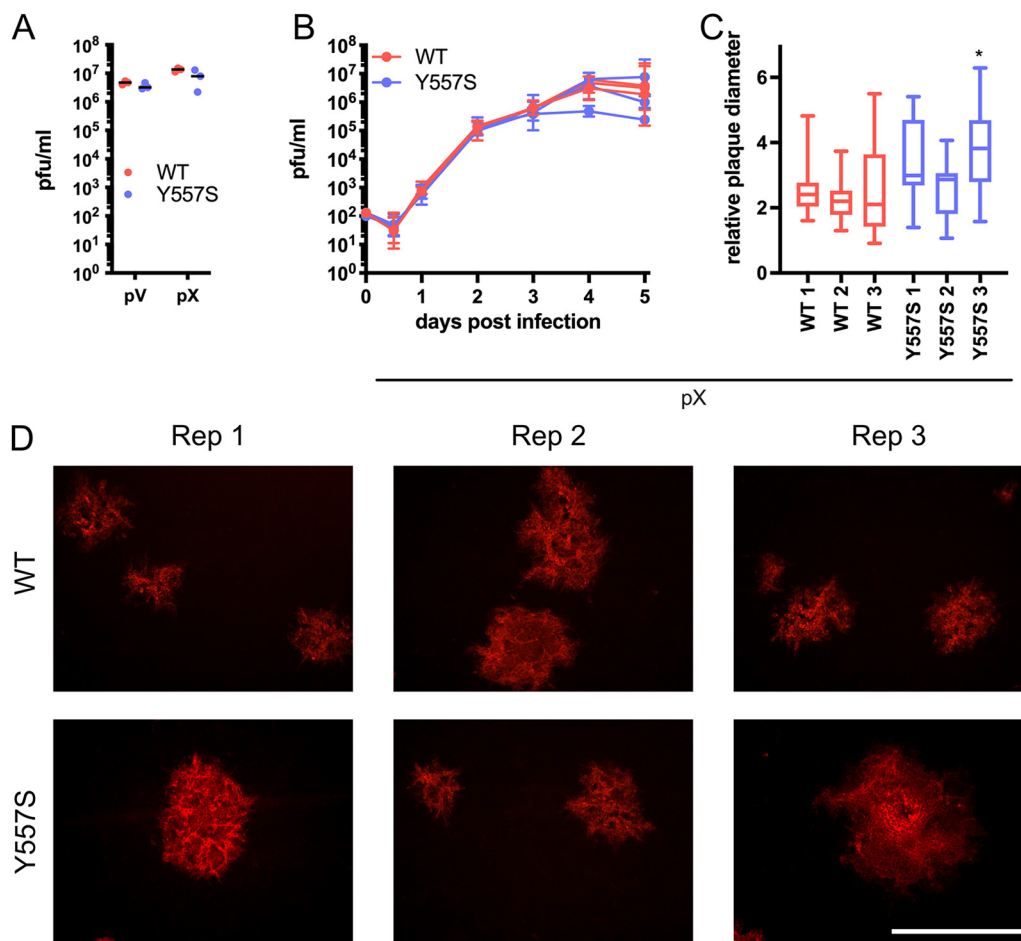
FIG 5 Y557S mutant replicates stably at later passages. (A) Viral endpoint titers for passaged WT and Y557S viruses. (B and C) Viral growth kinetics measured as multistep growth curves (B) and plaque size (C). Significances were calculated by two-way ANOVA followed by Šidák's multiple-comparison test for multistep growth curves and one-way ANOVA followed by Dunnett's multiple-comparison test for plaque size assays, respectively. An asterisk indicates significant ($P < 0.05$) differences in comparison to the WT for multistep growth curves and against WT replicate 1 for plaque size assays. (D) Plaque images taken at ×100 magnification of indicated viruses and passages. Scale bar, 500 μm.

cause unfavorable effects potentially culminating in lethal dysfunction. Similar to many other forms of cellular life, large DNA viruses such as HSV-1 encode replicative DNA polymerases with 3′–5′ exonuclease activity to increase replication fidelity and thus enable maintenance of large DNA genomes. While abrogation of exonuclease function has been reported to be lethal for HSV-1 in the past (5), we report successful reconstitution of all Pol mutants generated for the purpose of this study. However, we did observe a severe, progressive growth deficit in all Exo I mutants as well as in the Exo III Y577F mutant. This growth defect was explicit in single-focus measures as well as in multistep growth kinetics and titers that could be achieved over passaging. Genome/FFU ratios were shifted considerably toward more genomes per infectious unit for all Pol mutants except the Y557S mutant. This indicates that although DNA is efficiently replicated early after reconstitution, most of the progeny created by hypermutators are unfit to form infectious particles. Strikingly, Exo I and Y577F mutants could not maintain growth when usual transmission bottlenecks were applied. Passaging of these viruses required the transfer of substantial amounts of infected cells in each passage, whereas the WT and Y557S passed without difficulty through quite narrow bottlenecks. Despite our efforts, long-term survival of most Pol mutants was not achievable and pIII was typically the last point at which infectious foci could be observed. We suppose that the great speed at which mutations in Exo I and Y577F accumulate is the reason for the clearly suicidal phenotype we observe. Muller's ratchet is a concept that
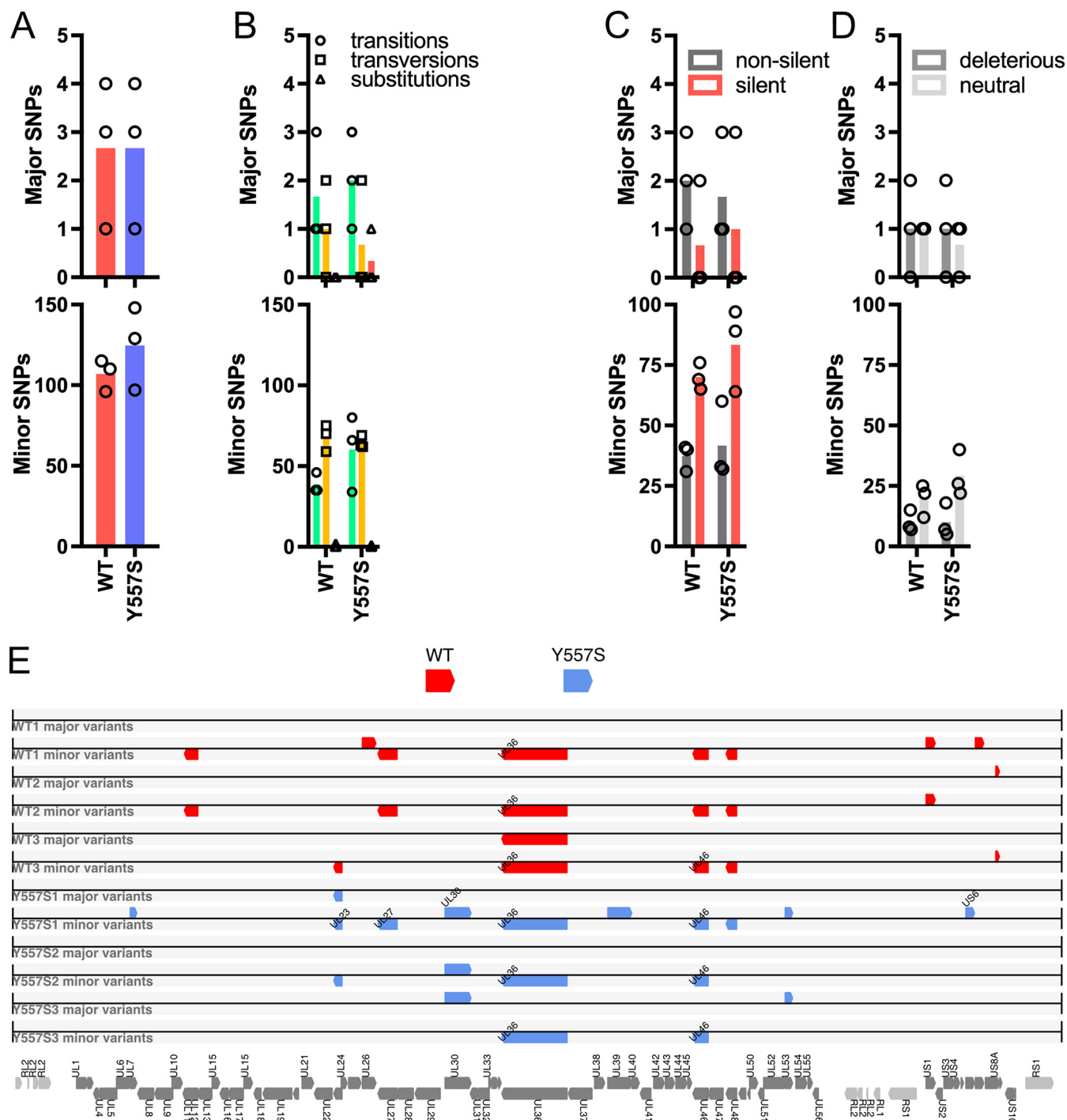
FIG 6 Stably replicating Y557S mutant accumulates more mutations than the WT. (A) SNP counts broken down to major and minor variants for WT and Y557S viruses at pX are shown. SNPs were included if the allele frequency was greater than 5%. (B) Major and minor SNPs of pX WT and Y557S viruses displayed according to the type of nucleotide exchange. (C) Major and minor SNPs in protein coding regions of pX WT and Y557S viruses grouped according to whether they lead to amino acid changes (nonsilent) or not (silent). (D) Nonsilent mutations from panel C into deleterious and neutral mutations according to SIFT predictions. (E) Genes affected by deleterious major or minor mutations, respectively, are depicted. Genes labeled with their respective name contain more than one deleterious mutation.

describes the accumulation of mutations in single genomes and the consequences that arise from an inability to clear deleterious mutations (28, 29). Even when recombination between different coinfecting viruses is limited, recombination can act on progeny genomes produced from the original infecting viruses, presenting the prime mechanism that unlinks beneficial from deleterious mutations. If the mutation rates, however, increase to the extent that

genomes produced in cells infected with a single virus are highly likely to feature at least one deleterious mutation, recombination between those genomes is less effective in purging these mutations and accumulation of deleterious mutations cannot be avoided. The most probable cause for the suicidal phenotype observed in Exo I and Y577F Pol mutants is the number and location of deleterious mutations which, in the case of these hypermutators, are highly enriched in viral populations by pIII. The gene sets featuring deleterious mutations are essential for productive viral replication and reproduction. No penetrant mutation in any of these important gene sets is found in the WT or Y557S at pIII. Although some mutations within essential genes can be found in the WT and Y557S at later passages, they remain far fewer than those of Exo I and Y577F mutants at pIII and they also are mainly featured in minor variants. Thus, this rapid and detrimental accumulation of mutations over few replication cycles could explain the suicidal phenotype of most Pol mutants described here. Based on their inability to perform proofreading, all our Exo I mutants should be uniformly depleted in their proofreading capability. Although all of these mutants present with similar phenotypes, the accumulation of mutations is not equal among them. Since some of the mutations we discovered in Exo I mutants map to UL30, the gene encoding Pol, it is not unlikely that strong selection for higher replication fidelity yields viruses that repair their replication fidelity in Pol domains other than Exo. Such a possibility has been previously described and could affect the accumulation of mutations we observed by pIII (30). This could explain the milder hypermutation observed for the D368A/E370A mutant. By pIII, this particular mutant population had gained 5 additional mutations within UL30 that could affect replication fidelity.

DNA mismatch repair proteins such as MSH2 and MLH1 are known to play important roles for efficient viral growth, MSH2 in general and MLH1 especially in primary human foreskin fibroblasts (24, 31). ICP8 interacts with MSH6 as well as UL12 and MSH2 colocalizes with HSV-1 replication sites, while MLH1 seems to be important for immediate early gene expression (31, 32). However, the cellular DNA mismatch repair machinery has so far not been shown to impact the mutation profile of HSV-1. Evidently, DNA repair mechanisms are not sufficient to rescue proofreading-deficient mutants.

Many molecular evolution studies observe a bias in transition/transversion substitution rates toward transitions (20, 33). It has been controversially discussed whether this bias is due to mutational bias (34–36) or selection bias (37–40). A mutational bias would suggest a bias toward transitions, because purine-to-pyrimidine changes and vice versa are sterically unfavorable and thus less likely to occur. A selection bias would presume that amino acid-changing mutations via transitions are more conservative than radical changes in the biochemical properties of replaced amino acids via transversions. Our study is not sufficiently powered to confirm or clearly reject any of these hypotheses. Despite that, it is tempting to speculate that the transition bias observed in our pIII sequencing data set, especially if compared to that of p0, is due to a mutation bias. Even if selection acts to preserve the biochemical integrity of viral proteins, the large bottleneck passaging performed here limits the effect of genetic drift and therefore many mutations are carried to subsequent passages. Furthermore, for our pX WT and Y557S populations, transversions are more common in minor variants, suggesting that selection favors radical amino acid changes. Clearly, more work needs to be done to untangle transition/transversion biases in HSV-1 Pol mutants.

The WT and Y557S are not just stable in their growth kinetics, as there is also some evidence for higher adaptability in the Y557S moderate hypermutator. This is indicated by larger plaque sizes and increased frequencies of syncytial plaque phenotypes, which have been shown to be selected for in Vero cell culture (41). Unfortunately, one Y557S replicate was harvested at a smaller population size, which might explain why this replicate featured fewer mutations than the other two. Overall, 10 passages provide insufficient evolutionary time to address differences in adaptability, so more research on this subject is necessary. We recently showed the higher adaptability of the MDV Pol Y547S mutant, the homolog of HSV-1 Y557S, which suggests that since Pol is highly conserved among alphaherpesviruses, the Y557S mutation can also confer evolutionary advantages (42).

Our results stand in contrast to previous reports on the lethal phenotype of Exo I mutants, specifically D358A (13). Although we cannot exclude that effects other than increased mutation rates contribute to the observed unfit phenotype of most Pol mutants described here, the initial ability of these mutants to replicate their genome and form infectious progeny, in combination with the extremely fast accumulation of mutations observed by us, strongly suggests that hypermutation caused by a lack of proofreading activity is the reason for the observed disability of Pol mutant viruses to sustain replication. While caution is mandated when directly comparing results between our study and previously published literature, there are a number of reasons that could explain these differences. The rapidly suicidal phenotype of Exo I mutants renders detection of virus recovery difficult. In our case, the green fluorescent protein (GFP) reporter gene carried by our viruses facilitated early identification of infectious foci. Although visible CPE developed for all viruses within 48 to 72 h following transfection, CPE typically disappeared as early as pI if not enough virus was transferred. In these cases, identification of infectious foci became impossible without fluorescence-based detection. Previously, the rescue of Pol mutants on Pol-complementing cells was reported to be possible; however, transfer to noncomplementing cells remained unsuccessful (13, 43). Although no description of the longer-term growth and stability of Pol mutants propagated on complementing cells is available, we assume that in such a case, both the WT polymerase expressed by the complementing cell and the mutant polymerase expressed by the virus would replicate virus genomes. This would likely stabilize virus replication, as abundant cellular expression of WT polymerase would enable high-fidelity replication of viral genomes. At the same time, DNA replication by the mutant polymerase would cause hypermutation but likely with less drastic effects because alternative high-fidelity replication is available. Upon transfer of Pol mutant viruses propagated on complementing cells to noncomplementing cells, these populations might already be weakened by previous hypermutation that interferes with their ability to replicate and cause CPE. Consequently, detection of these viruses might again be very difficult. Of course, many other factors, such as different virus strains, different methods employed in virus reconstitution, and different ways of assaying virus replication, could contribute to the difference in phenotypes observed for Pol mutants between our and previous studies. Of note, literature suggests that in the case of human cytomegalovirus (HCMV), exonuclease-deficient mutants are selected by their ganciclovir-resistant phenotype (44). Although HCMV is a betaherpesvirus and thus not directly related to HSV-1, the existence of viable HCMV variants that carry mutations within highly conserved exonuclease domains of viral Pol does support the notion that such exonuclease-deficient herpesvirus mutants are viable in principle.

In conclusion, we show that HSV-1 Exo mutants are viable but exhibit suicidal phenotypes early after reconstitution. Furthermore, we provide evidence that this phenotype is caused by a greatly increased accumulation of deleterious mutations in essential gene sets. Thus, the primary reason for the observed phenotype is drastically increased mutation rates due to a lack of exonucleolytic proofreading. Although the integrity of the exonuclease domains contained in Pol would in this case not be directly essential for the ability of HSV-1 to infect cells and form virus progeny, proofreading performed by the exonuclease is crucial to maintain genome integrity and thus is essential for maintaining virus replication in the long run. This would also make the exonuclease domain of the HSV-1 polymerase a possible target for future antiviral drug development. Lethal mutagenesis is an established concept in antiviral therapy (18) but is typically applied to RNA viruses that exist, in comparison to large DNA viruses, closer to a lethal error threshold (45–47). Since large DNA viruses employ their proofreading capabilities to replicate their genome with high fidelity (48, 49), lethal mutagenesis is difficult to achieve in the presence of proofreading. Therefore, inactivation of exonuclease domains might be key to antiviral treatments based on lethal mutagenesis for DNA viruses. In a recent paper, HSV-1 Pol and Exo were both described as potential targets for antiviral therapy, and the rapid decline of Exo-deficient populations observed by us generally supports such a strategy (50). Despite the strongly suicidal phenotype of most Pol mutants described here, we could identify the Exo III Y557S mutant as a stably replicating virus that replicated with slightly elevated mutation rates and potentially features higher adaptability than that of the WT. This stands in agreement with the

substantial remaining exonuclease activity reported for this mutant (9) and suggests that Y557S is a prime candidate for experimental studies on major aspects of viral evolution, such as antiviral resistance, immune evasion, spillover, and others. Higher mutation rates of moderate hypermutators could allow accelerated evolution (42) and would make studies on experimental evolution, a very time- and labor-intensive field, much more approachable in the future.

MATERIALS AND METHODS

Cells and viruses. Vero cells (ATCC CCL-81) were cultured in Dulbecco's modified eagle medium (DMEM; Pan Biotech) supplemented with 5 to 10% fetal calf serum (FCS), 100 IU/mL penicillin G (Carl Roth), and 100 μg/mL streptomycin (Carl Roth). All viruses used in this study were derived from HSV-1 F strain pYEbac102 kindly provided by Y. Kawaguchi, University of Tokyo, Japan (51). For easier detection of cellular virus infection, an immediately early cytomegalovirus (CMV) promoter-driven GFP was inserted into the Mini-F cassette of the virus construct.

Transfection. Vero cells were transfected using a standard polyethylenimine (PEI; Polysciences) transfection procedure (52). For transfection, 10 μL PEI (1 mg mL^{-1}) was diluted in 50 μL Opti-MEM (Thermo Fisher Scientific) and mixed with bacterial artificial chromosome (BAC) DNA (5 μg of BAC DNA in 50 μL of Opti-MEM). Following 25 min of incubation at room temperature, the DNA-PEI complex was added to a 90% confluent Vero cell monolayer, and one reaction mixture as described above was used per well in a 6-well plate. For transfection of 10-cm plates, an upscaled reaction (8-fold) was used. Cell culture medium was changed 4 h posttransfection.

Infection of cells and propagation of virus. Virus was propagated by transferring infected cell lysate (obtained by freezing and thawing of infected cells) to a confluent monolayer of uninfected Vero cells. When the CPE became apparent 2 to 3 days postinfection, virus was transferred to fresh cells as described above. To maintain growth of the D368A, E370A, D368A/E370A, and Y577F mutants, in each passage, one third of the cells in an infected dish had to be transferred to a new dish without addition of fresh cells. Cells were suspended using trypsin-EDTA (0.25% trypsin [Sigma-Aldrich], 0.5 mM EDTA [AppliChem] in phosphate-buffered saline [PBS]). In the case of Y557S and the WT, transfer of a small amount of supernatant (0.25% of the total volume) obtained from infected cell cultures was sufficient to maintain virus growth.

To monitor virus growth over passaging, HSV-1 was transfected in 6-well plates and supernatants were collected before passaging at 72 h posttransfection for passage 0 (p0) and at 48 h postinfection for subsequent passages I to V (pI to pV). From p0 to pI, all viruses were passaged by transferring one-third of the infected cells to a new dish without addition of fresh cells. From pI to pV, viruses were passaged on 10-cm dishes as described above. Prior to passaging, 1 mL of supernatant was collected for each virus and frozen at −80°C for at least 24 h. DNA was isolated from these cell-free virus stocks and used for qPCR as described below. The experiment was replicated three times, starting from independent transfections each time.

Virus titration and focus/plaque size assays. Since most Pol mutants fail to cause readily visible CPE by the early passages after reconstitution in Vero cell culture, we determined infectious virus particles as FFU either identified by the GFP carried in the BAC construct or by immunofluorescent staining (GFP is lost after 5 to 10 passages). Virus stocks were titrated by plating 10-fold serial dilutions on subconfluent Vero cells in 6-well dishes. Infectious foci were determined by counting fluorescent foci using a Zeiss Axio Vert.A1 inverted fluorescence microscope. Cells were transfected as described above or infected with 200 FFU per well using a 6-well plate. For p0, pictures were taken 72 h posttransfection, and for subsequent passages, pictures were taken 48 h postinfection using a Zeiss Axio Vert.A1 inverted fluorescence microscope. For the WT and the Y557S mutant, cell culture medium was replaced by a semisolid overlay of methylcellulose (0.75% methylcellulose in 1× DMEM supplemented with 5% FCS, 100 IU/mL penicillin G, 100 μg streptomycin, and 0.075% NaHCO$_3$) 1 h postinfection. For all other mutants, settling of transferred cells was allowed to occur before replacement of the medium 24 h postinfection. Focus size areas were measured with NIH Image J 1.52n software and converted to focus diameters relative to that of the WT of the respective passage (for early p0 and pIII viral populations) or to the WT at p0 (for later pX). As the GFP marker was readily lost after pX, plaques were stained using a cross-reactive simplex virus gB monoclonal antibody (C2D8) (53).

Cryopreservation of viruses. Cell-free virus was collected by directly freezing infected cell cultures at −80°C. To maximize virus titers, infected cell lysates were generated by freezing plates at −80°C, followed by thawing to release virus particles. Then, both supernatant and cells were used to create viral stocks, which were transferred immediately to –80°C and stored until further use.

DNA extractions for qPCR and transfection. Viral DNA was extracted, using the RTP DNA/RNA virus minikit (Stratec Molecular), from supernatant or from infected cell lysates (after freezing and thawing). Supernatants were cleared by centrifugation (1,000 × g, 5 min), and cell lysates were used entirely. DNA was extracted according to the manufacturer's instructions, with 400 μL of sample and the addition of 5 μL proteinase K (20 mg/mL) into the extraction tube. For the purpose of transfection (virus reconstitution), viral BAC DNA from *Escherichia coli* cultures was isolated using Qiagen's column-based midiprep kit according to the manufacturer's instructions.

Isolation of viral DNA for next-generation sequencing (NGS). Foci were picked by positioning a cell culture plate under a Zeiss Axio Vert.A1 inverted fluorescence microscope at ×50 magnification. A p200 pipette was used to pick infected cells and some supernatant in a volume of 50 μL. A total of 30 foci for each virus were collected. Viral DNA was extracted using the RTP DNA/RNA virus minikit (Stratec Molecular).

For pX of WT and Y557S, viral DNA was isolated by micrococcal nuclease DNA extraction (54). In brief, completely infected confluent 10-cm plates were harvested. Cell pellets were permeabilized twice in 5 mL of

permeabilization buffer (320 mM sucrose, 5 mM MgCl$_2$, 10 mM Tris-HCl [pH 7.5], 1% Triton X-100) by resuspension and centrifugation at 1,300 $\times$ *g* and 4°C. Pelleted nuclei were resuspended in 50 μL nuclei buffer (10 mM Tris-HCl [pH 7.5], 2 mM MgCl$_2$, 10% sucrose) and mixed with equal amounts of 2$\times$ nuclease buffer {40 mM PIPES [piperazine-*N*,*N*′-bis(2-ethanesulfonic acid)], 7% sucrose, 20 mM NaCl, 2% CaCl$_2$, 10 mM 2-mercaptoethanol, 200 μM phenylmethylsulfonyl fluoride [PMSF]} supplemented with 1 μL of RNase A (10 mg/mL) and 1.5 μL of micrococcal nuclease (2,000 gel units/μL; NEB). After incubation at 37°C for 90 min, the reaction was stopped by adding 2.4 μL of 0.5 M EDTA. Protein digestion was performed by adding 400 μL of digestion buffer (100 mM NaCl, 10 mM Tris-HCl [pH 8.0], 25 mM EDTA, 0.5% SDS) supplemented with 2.5 μL of proteinase K (20 mg/mL) at 50°C for 18 h. After three rounds of phenol-chloroform extraction, DNA was precipitated by adding 800 μL ethanol and 200 μL 7.5 M ammonium acetate to 400 μL of sample. After pelleting at 20,000 $\times$ *g* and 4°C for 20 min, pellets were washed with 70% ethanol and pelleted as described before. Air-dried pellets were dissolved in 70 μL of 10 mM Tris-HCl (pH 7.5).

Viral growth kinetics. For growth kinetics of pII viruses, approximately 1 $\times$ 10^6 Vero cells were infected with 200 FFU virus in triplicate using 6-well plates. For each time point, three replicate wells were harvested by freezing at −80°C every 12 h for 3 days. Viral DNA was isolated from 400 μL of sample (including supernatant and cells) and used for qPCR in duplicate reactions. For growth kinetics of pX viruses, Vero cells were infected at a multiplicity of infection (MOI) of 0.001 in 6-well plates in triplicate. Each time point and replicate consisted of one separate well. The respective wells were frozen to stop the infection at the indicated time points and thawed to create stocks, which were titrated by 10-fold serial dilutions. The medium was changed to a methylcellulose overlay 1 h postinfection and incubated at 37°C and 5% CO$_2$ until plaques formed. The plates were washed twice with PBS, fixed with 0.4% formaldehyde for 20 min, and stained with 0.75% crystal violet. Titers were calculated per milliliter of stock.

BAC mutagenesis. HSV-1 mutants were generated by en passant mutagenesis, a two-step Red-mediated recombination protocol (19). PCR products containing recombination-specific sites, the desired point mutation, an I-SceI recognition site, and a kanamycin resistance gene (*aphAI*) as a selection marker were generated and used to transform electrocompetent and recombination-competent *E. coli* carrying the HSV-1 F strain BAC. Arabinose-induced I-SceI expression initiated a double-strand break in the DNA, followed by homologous recombination to remove *aphAI*. Kanamycin-susceptible clones were selected and confirmed by restriction fragment length polymorphism analysis and Sanger sequencing of the relevant loci (19). (See Table S1 in the supplemental material for a list of all primers used for BAC mutagenesis). The UL30-Kan mutant used in Fig. 2E and F is the UL30 D368A *aphAI*-containing intermediate prior to resolution of *aphAI* cointegration.

PCR. PCRs were performed for Sanger sequencing, mutagenesis (using high-fidelity DNA polymerases such as S7 Fusion [Mobidiag] or PrimeStar [TaKaRa Bio]), and to determine the presence and orientation of specific sequences (using DreamTaq [Thermo Scientific] polymerase). PCRs were carried out in a total volume of 50 μL. All polymerases and reaction buffers were used according to the manufacturer's instructions. The NEB Tm Calculator (http://tmcalculator.neb.com) was used to calculate an annealing temperature that was suitable for both the polymerase and the respective primers (Table S1).

qPCRs were performed to quantify the amount of viral DNA in virus stocks by use of a TaqMan protocol. For the detection of viral DNA, primers and probe were designed to match a conserved region in UL30, the gene encoding the viral DNA polymerase. Standard curves were generated using HSV-1 BAC DNA of known concentration. PCRs were carried out in 20 μL with a 100 nM concentration of each primer and probe and 2 μL of sample DNA. Duplicate reactions were performed on an ABI 7500 fast real-time PCR machine (Thermo Fischer) using the SensiFast master mix (Bioline, Luckenwalde, Germany) with the following conditions: initial denaturation at 95°C for 180 s and then 35 cycles of denaturation for 15 s at 95°C, followed by primer annealing for 15 s at 55°C and elongation for 30 s at 68°C. Normalized gene copy numbers per milliliter of supernatant were calculated and provided for analysis.

NGS and target enrichment. Samples from every mutant at p0 and pIII (as well as pX for the Y557S mutant and the WT) underwent whole-genome DNA sequencing using the Illumina MiSeq platform. To this end, sequencing libraries were prepared using the NEBNext Ultra II DNA library prep kit (NEB). DNA fragmentation was performed by using a Covaris M220 focused ultrasonicator on 1 to 5 μg of extracted DNA that was diluted in up to 130 μL of 0.1$\times$ Tris-EDTA (TE) buffer. The size selection step of the NEBNext Ultra II DNA library prep protocol was performed for selection of fragments between 500 and 700 bp. Sequencing libraries for p0 and pIII samples were then enriched for HSV-1 genomic DNA using a myBaits hybridization capture for targeted NGS kit (Arbor Biosciences) with a custom-designed set of RNA probes to target the whole HSV-1 F strain genome (GenBank accession no. GU734771.1). The hybridization reaction was maintained for 20 h; enriched libraries were then recovered "off-bead" per the manufacturer's instructions, and the final PCR cleanup was performed using SPRI beads (AMPure XP beads; Beckman Coulter) at a ratio of 0.9. Final enriched libraries were pooled and loaded into the MiSeq instrument per Illumina's instructions.

The resultant Illumina sequencing data were processed with Trimmomatic v.0.39 (55) and mapped against an HSV-1 strain F-based reference (GU734771.1) using the Burrows-Wheeler Aligner v.0.7.17 (56). Since the sequence of the BAC-derived HSV-1 F strain virus differs slightly from the RefSeq entry (GU734771.1), an updated version of the reference was manually generated and deposited at GitHub (https://github.com/mmnascimento/HSV1polmutants). Mapping statistics were generated using Samtools v1.10 (57), and alignments were visualized using IGV v2.9.4 for Linux (58). For detection of single-nucleotide polymorphisms (SNPs), Freebayes, a Bayesian genetic variant detector (5), was used. All SNPs with a minimum mapping quality of 5, minimum count of 3, and minimum fraction of 0.01 were considered. Consensus sequences for each sample were obtained using BCFtools (57). All SNP-containing ORF sequences were extracted from these consensus genomes and translated using a custom-made script also deposited in the GitHub repository for this work (https://github.com/mmnascimento/HSV1polmutants).

SUPPLEMENTAL MATERIAL

Supplemental material is available online only.

SUPPLEMENTAL FILE 1, PDF file, 1.5 MB.

ACKNOWLEDGMENTS

REFERENCES

1. Gatherer D, Depledge DP, Hartley CA, Szpara ML, Vaz PK, Benko M, Brandt CR, Bryant NA, Dastjerdi A, Doszpoly A, Gompels UA, Inoue N, Jarosinski KW, Kaul R, Lacoste V, Norberg P, Origgi FC, Orton RJ, Pellett PE, Schmid DS, Spatz SJ, Stewart JP, Trimpert J, Waltzek TB, Davison AJ. 2021. ICTV virus taxonomy profile: Herpesviridae 2021. J Gen Virol 102:001673. https://doi.org/10.1099/jgv.0.001673.
2. Knopf CW, Weisshart K. 1988. The herpes simplex virus DNA polymerase: analysis of the functional domains. Biochim Biophys Acta 951:298–314. https://doi.org/10.1016/0167-4781(88)90100-5.
3. Larder BA, Kemp SD, Darby G. 1987. Related functional domains in virus DNA polymerases. EMBO J 6:169–175. https://doi.org/10.1002/j.1460-2075.1987.tb04735.x.
4. Wong SW, Wahl AF, Yuan PM, Arai N, Pearson BE, Arai K, Korn D, Hunkapiller MW, Wang TS. 1988. Human DNA polymerase alpha gene expression is cell proliferation dependent and its primary structure is similar to both prokaryotic and eukaryotic replicative DNA polymerases. EMBO J 7:37–47. https://doi.org/10.1002/j.1460-2075.1988.tb02781.x.
5. Gibbs JS, Weisshart K, Digard P, deBruynKops A, Knipe DM, Coen DM. 1991. Polymerization activity of an alpha-like DNA polymerase requires a conserved 3'-5' exonuclease active site. Mol Cell Biol 11:4786–4795. https://doi.org/10.1128/mcb.11.9.4786-4795.1991.
6. Hwang YT, Liu BY, Hong CY, Shillitoe EJ, Hwang CB. 1999. Effects of exonuclease activity and nucleotide selectivity of the herpes simplex virus DNA polymerase on the fidelity of DNA replication in vivo. J Virol 73:5326–5332. https://doi.org/10.1128/JVI.73.7.5326-5332.1999.
7. Hwang YT, Liu BY, Coen DM, Hwang CB. 1997. Effects of mutations in the Exo III motif of the herpes simplex virus DNA polymerase gene on enzyme activities, viral replication, and replication fidelity. J Virol 71:7791–7798. https://doi.org/10.1128/JVI.71.10.7791-7798.1997.
8. Hwang YT, Hwang CB. 2003. Exonuclease-deficient polymerase mutant of herpes simplex virus type 1 induces altered spectra of mutations. J Virol 77:2946–2955. https://doi.org/10.1128/jvi.77.5.2946-2955.2003.
9. Kuhn FJ, Knopf CW. 1996. Herpes simplex virus type 1 DNA polymerase. Mutational analysis of the 3'-5'-exonuclease domain. J Biol Chem 271:29245–29254. https://doi.org/10.1074/jbc.271.46.29245.
10. Baker RO, Hall JD. 1998. Impaired mismatch extension by a herpes simplex DNA polymerase mutant with an editing nuclease defect. J Biol Chem 273:24075–24082. https://doi.org/10.1074/jbc.273.37.24075.
11. Steitz TA. 1998. A mechanism for all polymerases. Nature 391:231–232. https://doi.org/10.1038/34542.
12. Hall JD, Orth KL, Sander KL, Swihart BM, Senese RA. 1995. Mutations within conserved motifs in the 3'-5' exonuclease domain of herpes simplex virus DNA polymerase. J Gen Virol 76:2999–3008. https://doi.org/10.1099/0022-1317-76-12-2999.
13. Lawler JL, Coen DM. 2018. HSV-1 DNA polymerase 3'-5' exonuclease-deficient mutant D368A exhibits severely reduced viral DNA synthesis and polymerase expression. J Gen Virol 99:1432–1437. https://doi.org/10.1099/jgv.0.001138.
14. Trimpert J, Groenke N, Kunec D, Eschke K, He S, McMahon DP, Osterrieder N. 2019. A proofreading-impaired herpesvirus generates populations with quasispecies-like structure. Nat Microbiol 4:2175–2183. https://doi.org/10.1038/s41564-019-0547-x.
15. Trimpert J, Osterrieder N. 2019. Herpesvirus DNA polymerase mutants—how important is faithful genome replication? Curr Clin Microbiol Rep 6:240–248. https://doi.org/10.1007/s40588-019-00135-2.
16. Bull JJ, Sanjuan R, Wilke CO. 2007. Theory of lethal mutagenesis for viruses. J Virol 81:2930–2939. https://doi.org/10.1128/JVI.01624-06.
17. Swanstrom R, Schinazi RF. 2022. Lethal mutagenesis as an antiviral strategy. Science 375:497–498. https://doi.org/10.1126/science.abn0048.
18. Hadj Hassine I, Ben M'hadheb M, Menéndez-Arias L. 2022. Lethal mutagenesis of RNA viruses and approved drugs with antiviral mutagenic activity. Viruses 14:841. https://doi.org/10.3390/v14040841.
19. Tischer BK, Smith GA, Osterrieder N. 2010. En passant mutagenesis: a two step markerless red recombination system. Methods Mol Biol 634:421–430. https://doi.org/10.1007/978-1-60761-652-8_30.
20. Fitch WM. 1967. Evidence suggesting a non-random character to nucleotide replacements in naturally occurring mutations. J Mol Biol 26:499–507. https://doi.org/10.1016/0022-2836(67)90317-8.
21. Whisnant AW, Jurges CS, Hennig T, Wyler E, Prusty B, Rutkowski AJ, L'Hernault A, Djakovic L, Gobel M, Doring K, Menegatti J, Antrobus R, Matheson NJ, Kunzig FWH, Mastrobuoni G, Bielow C, Kempa S, Liang C, Dandekar T, Zimmer R, Landthaler M, Grasser F, Lehner PJ, Friedel CC, Erhard F, Dolken L. 2020. Integrative functional genomics decodes herpes simplex virus 1. Nat Commun 11:2038. https://doi.org/10.1038/s41467-020-15992-5.
22. Sim NL, Kumar P, Hu J, Henikoff S, Schneider G, Ng PC. 2012. SIFT web server: predicting effects of amino acid substitutions on proteins. Nucleic Acids Res 40:W452–W457. https://doi.org/10.1093/nar/gks539.
23. Weller SK, Coen DM. 2012. Herpes simplex viruses: mechanisms of DNA replication. Cold Spring Harb Perspect Biol 4:a013011. https://doi.org/10.1101/cshperspect.a013011.
24. Packard JE, Dembowski JA. 2021. HSV-1 DNA replication-coordinated regulation by viral and cellular factors. Viruses 13:2015. https://doi.org/10.3390/v13102015.
25. Hilterbrand AT, Heldwein EE. 2019. Go go gadget glycoprotein!: HSV-1 draws on its sizeable glycoprotein tool kit to customize its diverse entry routes. PLoS Pathog 15:e1007660. https://doi.org/10.1371/journal.ppat.1007660.
26. Ahmad I, Wilson DW. 2020. HSV-1 cytoplasmic envelopment and egress. Int J Mol Sci 21:5969. https://doi.org/10.3390/ijms21175969.
27. Xu X, Che Y, Li Q. 2016. HSV-1 tegument protein and the development of its genome editing technology. Virol J 13:108. https://doi.org/10.1186/s12985-016-0563-x.
28. Muller HJ. 1964. The relation of recombination to mutational advance. Mutat Res 106:2–9. https://doi.org/10.1016/0027-5107(64)90047-8.
29. Jaramillo N, Domingo E, Munoz-Egea MC, Tabares E, Gadea I. 2013. Evidence of Muller's ratchet in herpes simplex virus type 1. J Gen Virol 94:366–375. https://doi.org/10.1099/vir.0.044685-0.
30. Tian W, Hwang YT, Lu Q, Hwang CB. 2009. Finger domain mutation affects enzyme activity, DNA replication efficiency, and fidelity of an exonuclease-deficient DNA polymerase of herpes simplex virus type 1. J Virol 83:7194–7201. https://doi.org/10.1128/JVI.00632-09.
31. Mohni KN, Mastrocola AS, Bai P, Weller SK, Heinen CD. 2011. DNA mismatch repair proteins are required for efficient herpes simplex virus 1 replication. J Virol 85:12241–12253. https://doi.org/10.1128/JVI.05487-11.
32. Taylor TJ, Knipe DM. 2004. Proteomics of herpes simplex virus replication compartments: association of cellular DNA replication, repair, recombination, and

chromatin remodeling proteins with ICP8. J Virol 78:5856–5866. https://doi.org/10.1128/JVI.78.11.5856-5866.2004.

33. Li W-H. 1985. Evolution of DNA sequences. In MacIntyre R (ed), Molecular evolutionary genetics. Springer, New York, NY.

34. Vogel F. 1972. Non-randomness of base replacement in point mutation. J Mol Evol 1:334–367. https://doi.org/10.1007/BF01653962.

35. Vogel F, Kopun M. 1977. Higher frequencies of transitions among point mutations. J Mol Evol 9:159–180. https://doi.org/10.1007/BF01732746.

36. Stoltzfus A, Norris RW. 2016. On the causes of evolutionary transition:transversion bias. Mol Biol Evol 33:595–602. https://doi.org/10.1093/molbev/msv274.

37. Wakeley J. 1996. The excess of transitions among nucleotide substitutions: new methods of estimating transition bias underscore its significance. Trends Ecol Evol 11:158–162. https://doi.org/10.1016/0169-5347(96)10009-4.

38. Rosenberg MS, Subramanian S, Kumar S. 2003. Patterns of transitional mutation biases within and among mammalian genomes. Mol Biol Evol 20:988–993. https://doi.org/10.1093/molbev/msg113.

39. Keller I, Bensasson D, Nichols RA. 2007. Transition-transversion bias is not universal: a counter example from grasshopper pseudogenes. PLoS Genet 3:e22. https://doi.org/10.1371/journal.pgen.0030022.

40. Lyons DM, Lauring AS. 2017. Evidence for the selective basis of transition-to-transversion substitution bias in two RNA viruses. Mol Biol Evol 34:3205–3215. https://doi.org/10.1093/molbev/msx251.

41. Kuny CV, Bowen CD, Renner DW, Johnston CM, Szpara ML. 2020. In vitro evolution of herpes simplex virus 1 (HSV-1) reveals selection for syncytia and other minor variants in cell culture. Virus Evol 6:veaa013. https://doi.org/10.1093/ve/veaa013.

42. Xing N, Höfler T, Hearn CJ, Nascimento M, Camps Paradell G, McMahon DP, Kunec D, Osterrieder N, Cheng HH, Trimpert J. 2022. Fast forwarding evolution—accelerated adaptation in a proofreading-deficient hypermutator herpesvirus. Virus Evol 8:veac099. https://doi.org/10.1093/ve/veac099.

43. Marcy AI, Yager DR, Coen DM. 1990. Isolation and characterization of herpes simplex virus mutants containing engineered mutations at the DNA polymerase locus. J Virol 64:2208–2216. https://doi.org/10.1128/JVI.64.5.2208-2216.1990.

44. Chen H, Beardsley GP, Coen DM. 2014. Mechanism of ganciclovir-induced chain termination revealed by resistant viral polymerase mutants with reduced exonuclease activity. Proc Natl Acad Sci U S A 111:17462–17467. https://doi.org/10.1073/pnas.1405981111.

45. Perales C, Domingo E. 2016. Antiviral strategies based on lethal mutagenesis and error threshold. Curr Top Microbiol Immunol 392:323–339. https://doi.org/10.1007/82_2015_459.

46. Domingo E, Perales C. 2018. Quasispecies and virus. Eur Biophys J 47:443–457. https://doi.org/10.1007/s00249-018-1282-6.

47. Domingo E, Perales C. 2019. Viral quasispecies. PLoS Genet 15:e1008271. https://doi.org/10.1371/journal.pgen.1008271.

48. Sanjuan R, Domingo-Calap P. 2016. Mechanisms of viral mutation. Cell Mol Life Sci 73:4433–4448. https://doi.org/10.1007/s00018-016-2299-6.

49. Sanjuan R, Nebot MR, Chirico N, Mansky LM, Belshaw R. 2010. Viral mutation rates. J Virol 84:9733–9748. https://doi.org/10.1128/JVI.00694-10.

50. DiScipio KA, Weerasooriya S, Szczepaniak R, Hazeen A, Wright LR, Wright DL, Weller SK. 2022. Two-metal ion-dependent enzymes as potential antiviral targets in human herpesviruses. mBio 13:e03226-21. https://doi.org/10.1128/mbio.03226-21.

51. Tanaka M, Kagawa H, Yamanashi Y, Sata T, Kawaguchi Y. 2003. Construction of an excisable bacterial artificial chromosome containing a full-length infectious clone of herpes simplex virus type 1: viruses reconstituted from the clone exhibit wild-type properties in vitro and in vivo. J Virol 77:1382–1391. https://doi.org/10.1128/jvi.77.2.1382-1391.2003.

52. Longo PA, Kavran JM, Kim MS, Leahy DJ. 2013. Transient mammalian cell transfection with polyethylenimine (PEI). Methods Enzymol 529:227–240. https://doi.org/10.1016/B978-0-12-418687-3.00018-5.

53. Borchers K, Ludwig H. 1991. Simian agent 8—a herpes simplex-like monkey virus. Comp Immunol Microbiol Infect Dis 14:125–132. https://doi.org/10.1016/0147-9571(91)90126-x.

54. Volkening JD, Spatz SJ. 2009. Purification of DNA from the cell-associated herpesvirus Marek's disease virus for 454 pyrosequencing using micrococcal nuclease digestion and polyethylene glycol precipitation. J Virol Methods 157:55–61. https://doi.org/10.1016/j.jviromet.2008.11.017.

55. Bolger AM, Lohse M, Usadel B. 2014. Trimmomatic: a flexible trimmer for Illumina sequence data. Bioinformatics 30:2114–2120. https://doi.org/10.1093/bioinformatics/btu170.

56. Li H, Durbin R. 2009. Fast and accurate short read alignment with Burrows-Wheeler transform. Bioinformatics 25:1754–1760. https://doi.org/10.1093/bioinformatics/btp324.

57. Danecek P, Bonfield JK, Liddle J, Marshall J, Ohan V, Pollard MO, Whitwham A, Keane T, McCarthy SA, Davies RM, Li H. 2021. Twelve years of SAMtools and BCFtools. Gigascience 10. https://doi.org/10.1093/gigascience/giab008.

58. Robinson JT, Thorvaldsdottir H, Wenger AM, Zehir A, Mesirov JP. 2017. Variant review with the Integrative Genomics Viewer. Cancer Res 77:e31–e34. https://doi.org/10.1158/0008-5472.CAN-17-0337.